

Article type : Supplement Article

## 1 INTRODUCTION

Bone is multifunctional, playing roles in mechanical support, protection, mineral homeostasis and hematopoiesis. Bone histomorphometry has been an essential technique for understanding tissue level events and bone adaptation physiology in basic and applied biomedical research.<sup>1-3</sup> Histomorphometry on a bone biopsy specimen has been the gold standard for clinical and pathologic evaluation.<sup>4</sup> Histologic assessment of bone from laboratory animals is routinely utilized as an outcome measure in scientific experiments.<sup>5</sup> Several limitations have been associated with bone histology such as time and cost effectiveness, difficulties with specimen preparation and sectioning. Additionally, the results are often limited to two-dimensional interpretations of the bone tissue.<sup>3,4</sup>

The use of three-dimensional technologies in biological and radiological imaging research has been advocated to replace two-dimensional systems.<sup>3,6,7</sup> However, newer systems need to be validated prior to broader acceptance. Bone histomorphometry is used to describe bone morphology, architecture and to quantify bone growth.<sup>1,2</sup> Histomorphometry applies stereological principles and thus a two-dimensional histological section can be estimated to account for changes in an entire three-dimensional structure.<sup>2</sup> Although this mathematical method of histomorphometry and stereology can be extrapolated with diagnostic significance in mineralized bone tissue experiments, bone imaged in three-dimensions can be better understood.<sup>2</sup> New imaging techniques and corresponding analysis such as micro-computed tomography can offer superior visualization and also overcome the limitations of two-dimensional methodologies.<sup>3,6,7</sup> A three-dimensional data set can reduce the effort required for sample preparation and therefore offers shorter time for evaluation/analysis and importantly, it is nondestructive.<sup>3</sup> Furthermore, micro-CT data sets can be subjected to traditional two dimensional analysis should that be desired.<sup>3,6,7</sup>

**This is the author manuscript accepted for publication and has undergone full peer review but has not been through the copyediting, typesetting, pagination and proofreading process, which may lead to differences between this version and the Version of Record. Please cite this article as doi: 10.1111/ocr.12265**

Recent animal studies have attempted to validate micro-CT as an alternative technique to histomorphometry for bone tissue turnover.<sup>3,7,8</sup> Many of these 3D studies have examined bone-implant integration.<sup>9-11</sup> In the current study, we examine a rodent model and compare the qualitative and quantitative alveolar bone modeling by using two methodologies – traditional two-dimensional histology and more recent three-dimensional imaging techniques that have been applied to human data sets.<sup>12</sup> Thus, the aim of this study was to examine the level of agreement of data obtained from high resolution *in vivo* micro-CT versus those obtained from traditional 2-D histomorphometry, to study bone modeling in an animal model.

## **MATERIALS and METHODS**

### **2.1 Study design**

Eleven rice rats were randomly selected from a larger ongoing experiment.<sup>13</sup> Details of the experimental design are described elsewhere. All animal procedures had IACUC approval. A pair of alizarin red and calcein green bone labels were administered *i.p.* The interval between each pair of alizarin or calcein labels was 7 days and the time interval between the second alizarin label and first calcein label was 14 weeks (Figure 1).

### **2.2 Histology evaluation**

To evaluate the alveolar bone modeling, the maxilla from each animal was dehydrated in graded alcohols and embedded in methyl methacrylate for analyses of bone labels. The embedded samples were cut into two halves through the intermaxillary suture with a diamond wire saw (Delaware Diamond Knives, Wilmington, DE). Approximately 6-8 consecutive undecalcified histological cross-sections (~70–80  $\mu\text{m}$ ) of the alveolar process and body of the maxilla from the molar region were obtained using a diamond wire saw (Delaware Diamond Knives, Wilmington, DE). These unstained histological sections were then mounted with Eukitt® (Quick-hardening mounting medium, 03989 Sigma-Aldrich, O. Kindler GmbH & Co.) for analysis under an epifluorescence bright field microscopy. Sites of bone formation or bone arrest close to the alveolar crest were quantified in the histological sections using Bioquant (Nashville, TN) imaging software (Figure. 2). Linear measurements were made from a second alizarin label to a second calcein label, which were administered about 15 weeks apart (Figure 1). The time at which the second alizarin and second calcein labels were administered also represent the time points at which micro-CT images were captured at T1 and T2, respectively. The measurements were made at the buccal or palatal alveolar crest in

regions where the labels were clearly visible as sharply demarcated lines (Figure 2). The bone growth represented the modeling activity at the alveolar crest, largely due to eruption of the molars and physiologic drift in the rodent model.

### 2.3 Micro-CT evaluation

*In vivo* micro-CT scans were obtained from the maxillary alveolar bone at two time points that corresponded to one week (T1) after the second alizarin and ~3 days (T2) after the second calcein label, i.e. at sacrifice (Figure 1). The images were acquired on a Siemens micro-CT scanner (Siemens Inveon Preclinical micro-CT, Knoxville, TN). All images were acquired under the following setting: 36.15  $\mu\text{m}$  pixel size, 401 projections, 675 ms exposure, 500  $\mu\text{A}$ , 80 kVP., with a cone angle of 14.6 degrees.

Three-dimensional reconstructions of the maxillae of the rats were evaluated using open source software as follows: Raw binary files from the micro-CT imaging were imported into Image J (Image processing and analyzes in java).<sup>14</sup> Regions of interest (limited to the maxilla from the scanned head) were defined, cropped in the Z-direction and saved as raw data. The cropped files were segmented and three-dimensional volumetric models were built by using ITK-SNAP (<http://www.itksnap.org>).<sup>15</sup> During the segmentation process, each two-dimensional projection was visualized in order to obtain and generate an accurate three-dimensional model. The volumetric models were then converted to surface models using Slicer software<sup>16</sup> (Figure 3).

The changes in bone size and thus bone modeling between the T1 and T2 models were measured in the superimposed 3D surface models.<sup>17,18</sup> The superimposition was obtained in two steps: 1) Approximation (as T1 and T2 micro-CT were obtained with different orientations), and 2) Voxel based registration. The region of reference used for registration was the maxilla without teeth, eliminating interference from the alveolar region which is subject to growth in the otherwise aged animals.<sup>17</sup>

Registered three-dimensional models were evaluated by two methods using tools available in the 3D Slicer: 1) Qualitatively by generating color maps (Figure 3,4) using a landmark based Q3DC tool (Figure 4). 2) Quantitative/landmark measurements, whereby fiducial points were placed on the 3D models (Figure 5) to measure bone modeling changes. In order to define the regions of interest, the same operator who prepared the 2D histology

sections identified identical sections in the 3D reconstruction. This was possible as landmarks such as the tooth crown and root shape could be used as references to precisely identify the same plane of section from the histology and in the corresponding 3D model. The fiducial points were marked on T1 and T2 3D models. The 3D Slicer software was used to compute the three-dimensional distance between the fiducial points. The qualitative/color maps and quantitative/landmark measurements based on 3D surface models were measured twice and the measurements were averaged.

Using the histologic and 3D methods described above, 60 paired measurements were obtained from the histological images and corresponding 3D images. The qualitative/quantitative agreement (difference in measurements) between methods was categorized as follows: poor ( $>150\mu\text{m}$ ), good ( $150$  to  $100\mu\text{m}$ ), or excellent ( $< 100\mu\text{m}$ ). The paired measurement from the histological sections, three-dimensional qualitative/color maps and quantitative/landmark based measurements were compared for agreement.

### **3 RESULTS**

The mean values of the histologic and 3D methods and the differences between micro-CT and histomorphometry measurements were obtained by subtracting the mean values obtained by histomorphometry from the mean value of micro-CT measurements. The difference in measurements between the methods revealed that of all measurements for qualitative/color maps (88.3%) and quantitative/landmark based (86.7 %) demonstrated excellent agreement, with less than  $100\mu\text{m}$  differences. Within these measurements of excellent accuracy, 43.3 and 51.7 % of the measurements showed less than  $<50\mu\text{m}$  differences for the qualitative and quantitative groups, respectively. While 10 and 8.3 % of the measurements displayed good agreement, only 1.7 and 5 % of those exhibited poor agreement for qualitative/color maps and quantitative/landmark based, respectively (Figure 6).

### **4 DISCUSSION**

Qualitative (color maps) and quantitative (linear measurement) modeling response in alveolar bone of a rodent model was compared by conventional two-dimensional histomorphometry and three-dimensional micro-CT analysis. Excellent agreement was found between the two methods. The evaluation of growth changes in the alveolar bone measured

on micro-CT images were in excellent agreement and thus provide an alternative method to histology-based morphometry, which is the current gold standard.

There are few studies in the literature comparing histomorphometry and micro-CT.<sup>3,6,8-10,19</sup> However, many of the studies were designed to reveal the response of surrounding bone tissue to an orthopedic or dental implant. Gabler et al.<sup>3</sup> found a high correlation between three-dimensional micro-CT and two-dimensional conventional histomorphometric quantification of the osseointegration of titanium implants. Although bone cells cannot be observed in micro-CT images, there are advantages to assessing data three dimensionally.<sup>8,10,19</sup> In the current study, approximately 6-8 consecutive cross-sections were obtained from one half of the maxilla. However, with micro-CT scans, it is possible to observe around 300 consecutive projections from the same area of interest.

In the clinical arena, superimposition of 3D data sets is becoming more common.<sup>20</sup> However, in patient images, the resolution of the images is ~5-10 fold less than micro-CT. With animal studies and the use of micro-CT, finer resolution can be obtained and a finer level of resolution is available to make measurements. Another unique aspect of the current technique is the ability to observe overlaying of three-dimensional models at two time points. Three-dimensional regional superimposition of a bone can provide visually, quantitative and qualitative evaluations of transverse, vertical, and anteroposterior skeletal and dental changes in jaws and other skeletal structures.<sup>17,18</sup>

During histological processing, biological samples are subjected to complex morphological deformations and staining artefacts. With the current methodology, *in vivo* micro-CT and *in vivo* labeling enabled a direct comparison of both micro-CT and histology. Hence, *in vivo* administered fluorochrome labels, which can allow for dynamic analysis of bone changes between T1 and T2 time points (Figure 4), and *in vivo* micro-CT scans at the same time point is part of the unique design of the current study. The results confirmed that over 86.7 % of the measurements had excellent agreement. Contrary to expectations, a number of the measurements had a difference of less than 50 $\mu$ m, which exceeded the level of agreement we anticipated.

Three-dimensional image registration based on the correspondence of voxels, particularly the regional registrations, have been recently validated by using regional superimposition of cone beam computed tomography scans.<sup>17,18</sup> However, there has been no

application and thus no validation of this method using micro-CT scans. We do not anticipate this to be an issue as micro-CT scans have a ~10 fold higher resolution. The current results support not only a reliable comparison between micro-CT and histomorphometry for linear measurements, but also demonstrate the accuracy of three-dimensional regional voxel-based registration with micro-CT scans.

The limitations of this study are as follows: There was a minor discrepancy (<1 week) between the bone labels that were measured and the time points at which the micro-CT scans were obtained. Given that the mineral apposition rate is low (<1 $\mu$ m/day), this would not have resulted in large differences. Currently, registration and overlay of 3D data sets is a time-consuming process that is not fully automated. As computation speed increases and algorithms become more robust, this limitation will likely be overcome. While it is not possible to obtain the exact same plane from histology and 3D images, it is likely that with multiple landmarks (crown, root, anatomical features), the plane of sections will be identical if not very close for all practical purposes.

## 5 CONCLUSION

A novel *in vivo* methodology was developed to obtain qualitative and quantitative data representing bone growth from micro-CT images and to compare them to two-dimensional histomorphometry, which remains the current gold standard. We found *in vivo* micro-CTs to be an excellent tool to precisely measure linear changes with appropriate software over time. The three-dimensional micro-CT qualitative and quantitative methods are reliable for measuring bone modeling changes and compare favorably to histology for the specific application described.

## LITERATURE

1. Burr DB, Allen MR. Basic And Applied Bone Biology. San Diego, CA: Elsevier Inc. 2014. 3 p.
2. Dempster DW, Compston JE, Drezner MK, Glorieux FH, Kanis JA, Malluche H, Meunier PJ, Ott SM, Recker RR, Parfitt AM. Standardized nomenclature, symbols, and units for bone histomorphometry: a 2012 update of the report of the ASBMR Histomorphometry Nomenclature Committee. *J Bone Miner Res* 2013;28:2-17.

3. Gabler C, Zietz C, Bieck R, Göhler R, Lindner T, Haenle M, Finke B, Meichsner J, Testrich H, Nowotnick M, Frerich B, Bader R. Quantification of osseointegration of plasma-polymer coated titanium alloyed implants by means of microcomputed tomography versus histomorphometry. *Biomed Res Int* 2015;2015:103-137.
4. Recker RR, Kimmel DB, Dempster D, Weinstein RS, Wronski TJ, Burr DB. Issues in modern bone histomorphometry. *Bone* 2011;49:955-64.
5. Robling AG, Turner CH. Mechanical signaling for bone modeling and remodeling. *Crit Rev Eukaryot Gene Expr* 2009;19:319-38.
6. Gielkens PF, Schortinghuis J, de Jong JR, Huysmans MC, Leeuwen MB, Raghoobar GM, Bos RR, Stegenga B. A comparison of micro-CT, microradiography and histomorphometry in bone research. *Arch Oral Biol* 2008;53:558-66
7. Holdsworth DW, Thornton MM. Micro-CT in small animal and specimen imaging. *Trends in Biotechnolog* 2002;20:34-39.
8. Park CH, Abramson ZR, Taba M Jr, Jin Q, Chang J, Kreider JM, Goldstein SA, Giannobile WV. Three-dimensional micro-computed tomographic imaging of alveolar bone in experimental bone loss or repair. *J Periodontol* 2007;78:273-81.
9. Gramanzini M, Gargiulo S, Zarone F, Megna R, Apicella A, Aversa R, Salvatore M, Mancini M, Sorrentino R, Brunetti A. Combined microcomputed tomography, biomechanical and histomorphometric analysis of the peri-implant bone: a pilot study in minipig model. *Dent Mater* 2016;32:794-806
10. Becker K, Klitzsch I, Stauber M, Schwarz F. Three-dimensional assessment of crestal bone levels at titanium implants with different abutment microstructures and insertion depths using micro-computed tomography. *Clin Oral Implants Res* 2017;28:671-676
11. Geng H, Todd NM, Devlin-Mullin A, Poologasundarampillai G, Kim TB, Madi K, Cartmell S, Mitchell CA, Jones JR, Lee PD. A correlative imaging based methodology for accurate quantitative assessment of bone formation in additive manufactured implants. *J Mater Sci Mater Med* 2016;27:112.
12. Graber TM, Vanardall RL, Vig K, Huang G. Orthodontics: Current Principles and Techniques. 6th Ed. St. Louis, MO: Elsevier Mosby, 2016, 99-153 p.

13. Exposto CR, Oz U, Callard JS, Allen MJ, Khurana H, Atri A, Mo X, Fernandez SA, Tatakis DN, Edmonds K, Westgate PM, Huja SS. Oncologic doses of zoledronic acid induce site specific suppression of bone modelling in rice rats. *Orthod Craniofac Res* 2017;20:83-88.
14. Rasband, W.S., ImageJ, U. S. National Institutes of Health, Bethesda, Maryland, USA, <http://imagej.nih.gov/ij/> 1997-2016.
15. Paul A. Yushkevich, Joseph Piven, Heather Cody Hazlett, Rachel Gimpel Smith, Sean Ho, James C. Gee, and Guido Gerig. User-guided three-dimensional active contour segmentation of anatomical structures: Significantly improved efficiency and reliability. *Neuroimage* 2006;31:1116-28.
16. Fedorov A., Beichel R., Kalpathy-Cramer J., Finet J., Fillion-Robin J-C., Pujol S., Bauer C., Jennings D., Fennessy F., Sonka M., Buatti J., Aylward S.R., Miller J.V., Pieper S., Kikinis R. three-dimensional Slicer as an Image Computing Platform for the Quantitative Imaging Network. *Magnetic Resonance Imaging* 2012;30:1323-41.
17. Ruellas AC, Huanca Ghislanzoni LT, Gomes MR, Danesi C, Lione R, Nguyen T, McNamara JA Jr, Cozza P, Franchi L, Cevidanes LH Comparison and reproducibility of 2 regions of reference for maxillary regional registration with cone-beam computed tomography. *Am J Orthod Dentofacial Orthop* 2016;149:533-42.
18. Ruellas AC, Yatabe MS, Souki BQ, Benavides E, Nguyen T, Luiz RR, Franchi L, Cevidanes LH. Three-dimensional Mandibular Superimposition: Comparison of Regions of Reference for Voxel-Based Registration. *PLoS One* 2016 23;11:e0157625
19. Gauthier O, Müller R, von Stechow D, Lamy B, Weiss P, Bouler JM, Aguado E, Daculsi G. In vivo bone regeneration with injectable calcium phosphate biomaterial: a three-dimensional micro-computed tomographic, biomechanical and SEM study. *Biomaterials* 2005;26:5444-53.
20. Chang YJ, Ruellas ACO, Yatabe MS, Westgate PM, Cevidanes LHS, Huja SS. Soft Tissue Changes Measured With Three-Dimensional Software Provides New Insights for Surgical Predictions. *J Oral Maxillofac Surg* 2017;75:2191-2201.



## FIGURE LEGENDS

**Figure 1** Time line of the experiment. The red arrows are alizarin and the green arrows are calcein administration time points. Pre and post micro-CT images were obtained at the 2<sup>nd</sup>, and 18<sup>th</sup> weeks.

**Figure 2** A histological section of the first molar under epifluorescence examination; A, The white arrow indicates bone formation between the red (alizarin) and green (calcein) labels on the buccal alveolar crest. The fine green lines, are generated in Bioquant Software and are the measurements of the distance between the two labels. The software provides one mean number to represent the bone growth at the alveolar crest B, Similarly, the blue arrow indicates bone formation similarly on the palatal side of the alveolar bone crest.

**Figure 3** Pre (T1) and post (T2) sacrifice 3D models. A, Occlusal view of three-dimensional pretreatment model. B Occlusal view of post sacrifice three-dimensional model. Right side maxillary 2<sup>nd</sup> and 3<sup>rd</sup> molars were extracted. C, Left sagittal registered and superimposed view. D Occlusal view of pre and post sacrifice three-dimensional registered and superimposed models (Voxel-based registration by Slicer software)

**Figure 4** Registered pre and post sacrifice time points and color maps/qualitative measurements. Vertical line indicates numerical equivalent of change in mm of every color as a color palate. Yellow is no change, and red is apposition of bone being above 0.125mm of change.

**Figure 5** Landmark identification in the pre and post sacrifice three-dimensional models. A, The representation of the location of histologic plane of section on the pre sacrifice 3D model. B, The representation of the location of histologic plane of section on the post sacrifice model. The thin white vertical lines correspond to the region and the plane of section from which the histologic section were obtained in the animal study. C, Point number 3 is the alveolar crest on the pre sacrifice model. D, Point number 4 is the alveolar crest on the post sacrifice model.

**Figure 6** The comparison of the agreement between qualitative/color maps and quantitative/landmark based measurements. The % of values with agreement (difference in measurements) between methods and were categorized as follows: poor (>150 $\mu$ m), good (150 to 100 $\mu$ m), or excellent (< 100 $\mu$ m).

**Figure 1**

**Figure 2**

**Figure 3**

**Figure 4**

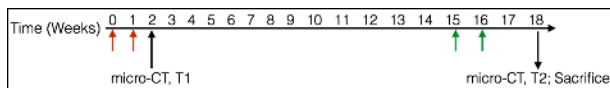
Author Manuscript

# Author Manuscript

**Figure 5**

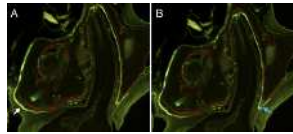
**Figure 6**

# Author Manuscript



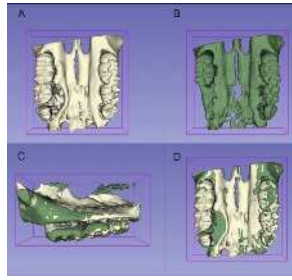
ocr\_12265\_f1.tif

# Author Manuscript



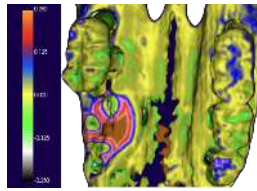
ocr\_12265\_f2.tiff

# Author Manuscript



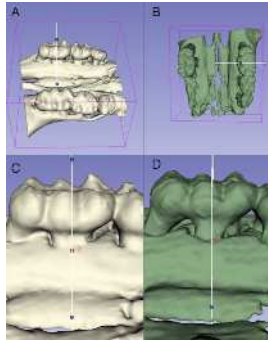
ocr\_12265\_f3.tiff

# Author Manuscript

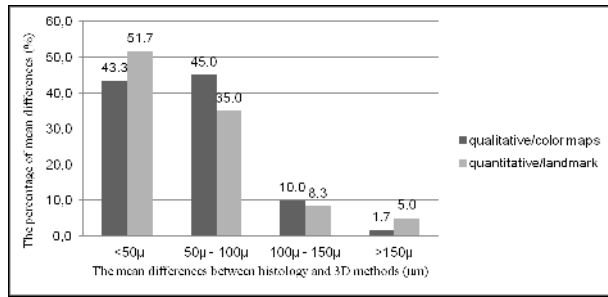


ocr\_12265\_f4.tiff





ocr\_12265\_f5.tiff



ocr\_12265\_f6.tif